Securing Image Super-Resolution Transmission with Relay Selection in Regenerative Relay Networks

Hien-Thuan Duong[†,#], Ca V. Phan[†], and Quoc-Tuan Vien[‡]
[†]Faculty of Electrical and Electronics Engineering, Ho Chi Minh City University of Technology and Education, Ho Chi Minh City 70000, Vietnam.
Email: {thuandh.ncs; capv}@hcmute.edu.vn.
[‡]Faculty of Science and Technology, Middlesex University, London NW4 4BT, UK. Email: q.vien@mdx.ac.uk.
[#]Faculty of Electronics and Telecommunications, Saigon University, Ho Chi Minh City 70000, Vietnam.
Email: thuan.duong@sgu.edu.vn.

***Abstract*—In the realm of wireless media, transmitting images is not without its risks, as eavesdroppers could potentially intercept and strive to retrieve images that are being sent. The study introduces a secure image cooperative transmission over a Rayleigh fading channel. In this setup, a user named Alice ($\mathcal{A}$) sends an image with great resolution to another user, Bob ($\mathcal{B}$), with the assistance of a relay, ($\mathcal{R}$), while an eavesdropper, Eve ($\mathcal{E}$), might be trying to listen in. To save transmission bandwidth, $\mathcal{A}$ reduces the size of the original high-resolution images. $\mathcal{B}$ then applies image super-resolution techniques to recreate the quality of high-resolution images from these downscaled versions. The security of the image is protected over wireless communication by using Random Linear Network Coding (RLNC) at both $\mathcal{A}$ and $\mathcal{R}$ to conceal the image into a reference image from the shared image datastore. The simulation shows that SCR (Secure Image Cooperative Relaying) yields a markedly improved output at $\mathcal{B}$ compared to $\mathcal{E}$ due to $\mathcal{E}$'s lack of knowledge regarding the coefficient matrices and reference images employed at $\mathcal{A}$ and $\mathcal{R}$. Additionally, relay selection strategies can be applied to enhance SCR's functionality.**

***Index Terms*—Image communication, Deep learning, ISR, RLNC, Cooperative communication, Decode and forward, Relay selection.**

I. Introduction

Many wireless network architectures have incorporated cooperative interactions, where relay nodes can be utilized for boosting system throughput and network coverage while also enhancing the quality of the signal and increasing gains in spatial diversity [1], [2]. In various relay networks, it is crucial to consider relay selection mechanisms to enhance network performance. A variety of relay selection techniques have been explored, aiming to improve various aspects such as reliability, efficiency, and overall throughput of the network. In [3], [4], the opportunistic relay selection approach is based on the instantaneous channel's measurements. Other selection schemes follow the threshold requirements of channels [5], where relays are chosen when they meet the necessary threshold. Adaptive relay selection techniques involve choosing a relay only when the connection between the source and destination weakens due to channel fluctuations [6].

Network coding (NC) has been applied to wireless communications, and a number of NC-based protocols have been developed for popular relay channel types, including broadcast channels [7], multicast channels [8], and relay-assisted bidirectional channels [9]. Furthermore, by restricting the degrees of freedom (decoding skills) that eavesdropper(s) can access, Random Linear NC (RLNC) can safeguard the connection [10].

Graphic language is ubiquitous in daily life, and one of the numerous scientific challenges is ensuring the security and quality of high-resolution image transmission across a lossy, bandwidth-limited wireless channel. Conventionally, the combined source and channel coding technique for image transmission was investigated in [11], [12]. In recent years, the process known as ISR (Image Super-Resolution) [13], [14], which uses deep learning techniques to generate one or more high-resolution images from one or more low-resolution observations, has attracted significant interest from scholars due to its superior performance.

Cryptography and information concealment are the two primary types of image security approaches for ensuring image privacy. Cryptography requires extensive computation, and some encryption methods have been studied in [15]. There are two types of information concealment techniques: steganography and watermarking, which limit the amount of hidden secret information but are less complex than encryption techniques [16].

In this paper, we extend the secure image cooperative transmission protocol from [17], which only considers an AWGN channel and a single relay, to include an opportunistic relay selection mechanism based on the optimal end-to-end path criterion [3], [4] for the flat Rayleigh fading channel.

The document's remaining sections are organized as follows: The multi-relay cooperative network under consideration, with DF relaying and relay selection, is described in Section II. We describe secure image cooperative transmission with relay selection in Section III. Section IV presents the simulation results and discussion. Section V concludes the paper.

II. System Model

As indicated in Fig. 1, the components of the system model include one source ($\mathcal{A}$), one destination ($\mathcal{B}$), one passive eavesdropper ($\mathcal{E}$), and M relays ($\mathcal{R}k$, where $k \in 1, 2, \ldots, M$).

Each node is equipped with a single antenna and is located at $(x\mathcal{Z}, y_{\mathcal{Z}})$, where $\mathcal{Z} \in \mathcal{A}, \mathcal{R}, \mathcal{B}, \mathcal{E}$. Independent identically distributed flat Rayleigh fading channels are used to model the channels between two nodes, and additive white Gaussian noise (AWGN) is present at the receiving nodes. Due to the half-duplex nature of the relays, two time periods are involved in the transmission of information. $\mathcal{A}$ uses the first time period to broadcast its message. In the second period, one relay, $\mathcal{R}_m$ $(m \in 1, 2, \ldots, M)$, is selected to decode the received signal, reprocess it, and retransmit it to $\mathcal{B}$. The instantaneous SNR or channel state information (CSI) of each hop is used by relay selection algorithms. Let us denote $\gamma_{\mathcal{A}\mathcal{R}_m}$ and $\gamma_{\mathcal{R}_m\mathcal{B}}$ as the instantaneous SNR of the $\mathcal{A} - \mathcal{R}_m$ and $\mathcal{R}_m - \mathcal{B}$ links, respectively. The relay that was chosen based on criterion of [3], [4], the best path connecting between $\mathcal{A}$ and $\mathcal{B}$, can be written as

$$\mathcal{R}_b = \arg\max_{\mathcal{R}_m} \{\min(\gamma_{\mathcal{A}\mathcal{R}_m}, \gamma_{\mathcal{R}_m\mathcal{B}})\} \tag{1}$$

where $\mathcal{R}_b$ is the selected Relay and $b \in 1, 2, ..., M$. We assume that all relays are situated in close proximity to one another (optimal clustering) [18]. Compared to the distance between the relays and the nodes $\mathcal{A}$, $\mathcal{B}$, and $\mathcal{E}$, the distance between any two relays is insignificant. Therefore, the selected relay among them is located at $(x_{\mathcal{R}}, y_{\mathcal{R}})$. In the following section, the chosen relay based on Eq. (1) will simply be referred to as "Relay" and denoted as $\mathcal{R}$ instead of $\mathcal{R}_b$ for simplicity.

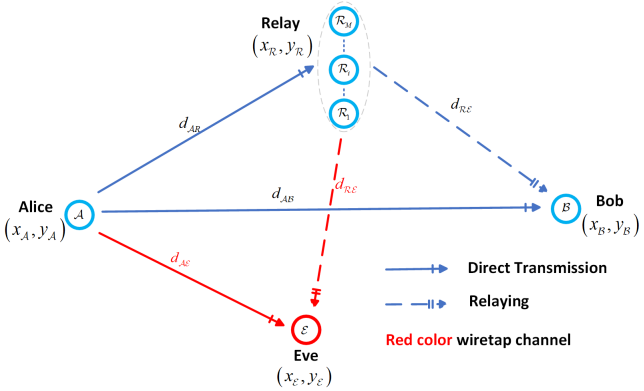

Fig. 1. System model of secure image communications in DF Relay Selection.

III. Secure Image Cooperative Transmission with Relay Selection

This study uses the same secure cooperative relaying protocol for image super-resolution protocol as that described in [17] with the impact of Rayleigh fading and relay selection scheme.

In the first time slot, $\mathcal{A}$ downscales the original HR (High Resolution) image, $\mathbf{I}_{\mathcal{A}}^{(HR)}$ of size $P \times Q \times 3$, into an LR (Low Resolution) version, $\mathbf{I}_{\mathcal{A}}^{(LR)}$ of size $P' \times Q' \times 3$, using bicubic interpolation to reduce the amount of transmission bandwidth required, where ϵ is a scaling factor, $P' = \lceil P/\epsilon \rceil$ and $Q' = \lceil Q/\epsilon \rceil$. $\mathbf{I}_{\mathcal{A}}^{(LR)}$ is encoded using RLNC for security reasons by combining the LR picture with the reference image, $\mathbf{I}_{\mathcal{A}}^{(ref)}$, which is randomly selected from the common image datastore, $\mathfrak{Q}$, the image that has been encoded at $\mathcal{A}$, can be obtained by

$$\mathbf{I}_{\mathcal{A}}^{(enc)} = \mathbf{R}_{\mathcal{A},1} \circ \mathbf{I}_{\mathcal{A}}^{(LR)} + \mathbf{R}_{\mathcal{A},2} \circ \mathbf{I}_{\mathcal{A}}^{(ref)}, \tag{2}$$

where $\mathbf{R}_{\mathcal{A},i}$, $i \in \{1, 2\}$, of size $P' \times Q' \times 3$ are RLNC matrix coefficients at $\mathcal{A}$, and $\circ$ indicates the Hadamard product, or element-wise multiplication, of two matrices. $\mathbf{I}_{\mathcal{A}}^{(enc)}$ is transformed into a binary stream and then various signal processing techniques, such as channel coding, digital modulation are applied to transmit over Rayleigh fading channel. Let $s_{\mathcal{A}}$ denotes modulated symbol at $\mathcal{A}$, the received signal at $\mathcal{R}$, $\mathcal{B}$ and $\mathcal{E}$ in first period of time can be written as

$$r_{\mathcal{R}}^{(1)} = \frac{h_{\mathcal{A}\mathcal{R}} s_{\mathcal{A}}}{d_{\mathcal{A}\mathcal{R}}^{\beta}} + n_{\mathcal{R}}^{(1)} \tag{3}$$

$$r_{\mathcal{B}}^{(1)} = \frac{h_{\mathcal{A}\mathcal{B}} s_{\mathcal{A}}}{d_{\mathcal{A}\mathcal{B}}^{\beta}} + n_{\mathcal{B}}^{(1)} \tag{4}$$

where $h_{\mathcal{A}\mathcal{Z}}$, $d_{\mathcal{A}\mathcal{Z}}$ with $\mathcal{Z} \in \{\mathcal{R}, \mathcal{B}, \mathcal{E}\}$ are Rayleigh fading channel gain distance between $\mathcal{A}$ and $\mathcal{Z}$, respecxtively. β is a factor of path loss. AWGN noise with zero mean and variation of $\sigma_{\mathcal{Z},1}^2$ at $\mathcal{Z}$ is represented by $n_{\mathcal{Z}}^{(1)}$. The received signal at selected relay $\mathcal{R}$ as Eq.(3) is applied signal processing such as equalization, digital demodulation and channel decoding to recover the transmitted binary stream from $\mathcal{A}$. The recovered binary stream is then convert to image format and use the pretrained DnCNN network [19], a deep neural network, to minimize noise of the image. Let $\bar{\mathbf{I}}_{\mathcal{R}}^{(1)}$ represents the image that has been denoised at $\mathcal{R}$. Chosen Relay may estimate the original LR image, $\mathbf{I}_{A}^{(ref)}$, using the Eq.(5) with the help of $\mathcal{A}$'s shared reference picture, $\mathbf{I}_{A}^{(ref)}$, and the RLNC coefficient matrices, $\mathbf{R}_{\mathcal{A},1}$ and $\mathbf{R}_{\mathcal{A},2}$

$$\hat{\mathbf{I}}_{\mathcal{R}}^{(1)} = \left(\bar{\mathbf{I}}_{\mathcal{R}}^{(1)} - \mathbf{R}_{\mathcal{A},2} \circ \mathbf{R}_{\mathcal{A}}^{(ref)}\right) \oslash \mathbf{R}_{\mathcal{A},1}, \tag{5}$$

where $\oslash$ represents division of two matrices element by element. During the second time slot, $\mathcal{R}$ uses the same reference picture, $\mathbf{I}_{\mathcal{A}}^{(ref)}$, and random coefficient matrices, $\mathbf{R}_{\mathcal{A},k}$, $k \in \{1, 2\}$ of RLNC that is used at $\mathcal{R}$, so that we can apply the diversity receiving techniques such as MRC, EGC, SC $\mathcal{B}$ at in the second time slot. Noted that, a reference photo and random coefficient matrix RLNC is used at $\mathcal{R}$ can be different from which used at $\mathcal{A}$, this case will be investigated in another article. The image encoded with RLNC can have the following expression

$$\mathbf{I}_{\mathcal{R}}^{(enc)} = \mathbf{R}_{\mathcal{A},1} \circ \hat{\mathbf{I}}_{\mathcal{R}}^{(1)} + \mathbf{R}_{\mathcal{A},2} \circ \mathbf{I}_{\mathcal{A}}^{(ref)}, \tag{6}$$

Before being sent over a fading channel, the RLNC-encoded image, $\mathbf{I}_{\mathcal{R}}^{(enc)}$, is processed in the same way as at $\mathcal{A}$, including being converted to binary stream, channel encoded, and modulated. Let $s_{\mathcal{R}}$ be modulated symbol that transmits to $\mathcal{B}$ and being eavesdropped by $\mathcal{E}$ in the second time period. The signal that was received at $\mathcal{B}$ and $\mathcal{E}$ can be expressed as

$$r_{\mathcal{B}}^{(2)} = \frac{h_{\mathcal{R}\mathcal{B}} s_{\mathcal{R}}}{d_{\mathcal{R}\mathcal{B}}^{\beta}} + n_{\mathcal{B}}^{(2)} \tag{7}$$

$$r_{\mathcal{E}}^{(2)} = \frac{h_{\mathcal{RE}} s_{\mathcal{R}}}{d_{\mathcal{RE}}^{\beta}} + n_{\mathcal{E}}^{(2)} \tag{8}$$

For SDT (Secure Direct Transmission) protocol, $\mathcal{B}$ receives signal in Eq.(4) will use ZF (Zero Forcing) equalization, demodulation and channel decoding via Viterbi algorithms to recover the transmitted binary stream from $\mathcal{A}$. After that, it is converted to image format then denoised by DnCNN [19]. The estimated original LR image at $\mathcal{B}$, $\hat{\mathbf{I}}_{\mathcal{B}}^{(1)}$, can be expressed as

$$\hat{\mathbf{I}}_{\mathcal{B}}^{(1)} = \left(\bar{\mathbf{I}}_{\mathcal{B}}^{(1)} - \mathbf{R}_{\mathcal{A},2} \circ \mathbf{I}_{\mathcal{A}}^{(ref)}\right) \oslash \mathbf{R}_{\mathcal{A},1}, \tag{9}$$

where $\bar{\mathbf{I}}^{(1)}$ is the estimated image following denoising. Following RLNC-decoding, by Using the freely accessible IAPR TC-12 Benchmark [20] data sets as training data, $\mathcal{B}$ employs the VDSR ISR architecture [13] to recover the whole pixel count of the original HR image. The HR image that $\mathcal{B}$ receives in the initial time slot can be acquired as

$$\hat{\mathbf{I}}_{\mathcal{B}}^{(HR,1)} = \nabla_{\epsilon}(\hat{\mathbf{I}}_{\mathcal{B}}^{(1)}), \tag{10}$$

here, the ISR algorithm to reconstruct the HR pictures with scaling factor ϵ is represented by the symbol $\nabla_{\epsilon}(\cdot)$.

For SRT (Secure Relaying Transmission) protocol, $\mathcal{B}$ receives signal in Eq.(4) and Eq.(7) will apply the diversity receiving schemes. The equalization of MRC, EGC, and SC can be stated as

$$\hat{r}_{\mathcal{B}.\mathcal{MRC}}^{(2)} = h_{\mathcal{AB}}^{*} r_{\mathcal{B}}^{(1)} + h_{\mathcal{RB}}^{*} r_{\mathcal{B}}^{(2)} \tag{11}$$

$$\hat{r}_{\mathcal{B}.\mathcal{EGC}}^{(2)} = e^{-j\angle h_{\mathcal{AB}}} r_{\mathcal{B}}^{(1)} + e^{-j\angle h_{\mathcal{RB}}} r_{\mathcal{B}}^{(2)} \tag{12}$$

$$\hat{r}_{\mathcal{B}}^{(2)} = \begin{cases} h_{\mathcal{AB}}^{-1} r_{\mathcal{B}}^{(1)} & if\ \gamma_{\mathcal{B}}^{(1)} > \gamma_{\mathcal{B}}^{(2)} \\ h_{\mathcal{RB}}^{-1} r_{\mathcal{B}}^{(2)} & if\ \gamma_{\mathcal{B}}^{(2)} > \gamma_{\mathcal{B}}^{(1)} \end{cases} \tag{13}$$

where instantaneous SNRs for the $\mathcal{A}-\mathcal{B}$ and $\mathcal{R}-\mathcal{B}$ channels are denoted by $\gamma_{\mathcal{B}}^{(1)}$ and $\gamma_{\mathcal{B}}^{(2)}$, respectively. Following their equalization, the signals will be modulated, channel decoded (using the Viterbi Algorithm), and formatted as an estimated image. DnCNN network [19] is used to denoise the estimated image, resulting in $\bar{\mathbf{I}}_{\mathcal{B}}^{(2)}$. $\mathcal{B}$ can use the RLNC method to retrieve the LR image that was transmitted from Relay.

$$\hat{\mathbf{I}}_{\mathcal{B}}^{(2)} = \left(\bar{\mathbf{I}}_{\mathcal{B}}^{(2)} - \mathbf{R}_{\mathcal{A},2} \circ \mathbf{I}_{\mathcal{A}}^{(ref)}\right) \oslash \mathbf{R}_{\mathcal{A},1}. \tag{14}$$

$\mathcal{B}$ uses an VDSR framework [13] to transform an LR received image into an HR original image

$$\hat{\mathbf{I}}_{\mathcal{B}}^{(HR,2)} = \nabla_{\epsilon}(\hat{\mathbf{I}}_{\mathcal{B}}^{(2)}). \tag{15}$$

For SCR (Secure Cooperative Relaying) protocol, $\mathcal{B}$ overlays $\hat{\mathbf{I}}_{\mathcal{B}}^{(HR,1)}$ in Eq.(10) and $\hat{\mathbf{I}}_{\mathcal{B}}^{(HR,2)}$ in Eq.(15) to create a blended image, merging the pictures that were recovered from the two time periods.

$$\hat{\mathbf{I}}_{\mathcal{B}}^{(HR)} = \alpha_1 \hat{\mathbf{I}}_{\mathcal{B}}^{(HR,1)} + \alpha_2 \hat{\mathbf{I}}_{\mathcal{B}}^{(HR,2)}, \tag{16}$$

The fraction of the i-th HR picture in the merging image is shown by α_i where i is among $\{1,2\}$. Which is also called Alpha blending factor [21].

The processing procedure at $\mathcal{E}$ is the same those at $\mathcal{B}$ in both time slots. The only difference is $\mathcal{A}$ and $\mathcal{R}$ do not share the reference image and RLNC matrix to $\mathcal{E}$. In order to decode the original picture in the first and second time slots, $\mathcal{E}$ tries to estimate the reference image, or $\hat{\mathbf{I}}_{\mathcal{A}}^{(ref)}$, and the RLNC coefficient matrices, or $\{\hat{\mathbf{R}}_{\mathcal{A},1}, \hat{\mathbf{R}}_{\mathcal{A},2}\}$. The encoded-RLNC images will be

$$\hat{\mathbf{I}}_{\mathcal{E}}^{(1)} = \left(\bar{\mathbf{I}}_{\mathcal{E}}^{(1)} - \hat{\mathbf{R}}_{\mathcal{A},2} \circ \hat{\mathbf{I}}_{\mathcal{A}}^{(ref)}\right) \oslash \hat{\mathbf{R}}_{\mathcal{A},1}, \tag{17}$$

$$\hat{\mathbf{I}}_{\mathcal{E}}^{(2)} = \left(\bar{\mathbf{I}}_{\mathcal{E}}^{(2)} - \hat{\mathbf{R}}_{\mathcal{R},2} \circ \hat{\mathbf{I}}_{\mathcal{R}}^{(ref)}\right) \oslash \hat{\mathbf{R}}_{\mathcal{R},1}. \tag{18}$$

where the denoised images for the first and second time slots, respectively, are marked by $\bar{\mathbf{I}}_{\mathcal{E}}^{(1)}$ and $\bar{\mathbf{I}}_{\mathcal{E}}^{(2)}$. Next, in the i-th time slot, where $i \in \{1,2\}$, $\mathcal{E}$ uses VDSR ISR [13] to recover the entire extent of the HR original picture, as

$$\hat{\mathbf{I}}_{\mathcal{E}}^{(HR,i)} = \nabla_{\epsilon}(\hat{\mathbf{I}}_{\mathcal{E}}^{(i)}). \tag{19}$$

Consequently, the image that was obtained from both time periods are blended in a similar way at $\mathcal{E}$.

$$\hat{\mathbf{I}}_{\mathcal{E}}^{(HR)} = \hat{\alpha}_1 \hat{\mathbf{I}}_{\mathcal{E}}^{(HR,1)} + \hat{\alpha}_2 \hat{\mathbf{I}}_{\mathcal{E}}^{(HR,2)}, \tag{20}$$

where $\hat{\alpha}_i$, $i \in \{1,2\}$, represents the estimated Alpha blending fraction of the i-th HR image in the composite image at $\mathcal{E}$.

IV. Simulation Results

The performance of the proposed approach is assessed using two performance metrics: the peak signal-to-noise ratio (PSNR) [22] and the structural similarity index measure (SSIM) [23].

In this simulation, MATLAB is utilized for both training and validation. The VDSR ISR [13] is trained using 20,000 naturally occurring static images from the IAPR TC-12 benchmark [20]. The network consists of 20 convolutional layers, with 64 patches per image, and an image patch size of 41 x 41. The image input layer has 64 3-by-3 filters and the penultimate layer is a convolutional layer with a single 3-by-3-by-64 filter. The middle layers consist of 18 alternating convolutional and rectified linear unit (ReLU) layers. The final layer calculates the mean square error between the residual image and network prediction. Stochastic gradient descent with momentum optimization is used to train the VDSR ISR network, with the following hyperparameters: The L2-norm method enables gradient clipping with a gradient threshold of 0.01. Starting at 0.1, the learning rate is reduced by a factor of 10 every 10 epochs, with a maximum of 100 epochs. The momentum value is set to 0.9. The validation method uses 20 of the unedited images in Fig.2, obtained using MATLAB's Image Processing Toolbox. In this simulation, the Rayleigh fading channel is employed. BPSK modulation and convolutional coding with generators $[111; 101]$ are used. The following node locations are evaluated: $\mathcal{B}$ is at $(0,3)$, and $\mathcal{A}$ is at $(0,0)$. $\mathcal{R}$ and $\mathcal{E}$ are positioned in the middle, at $(1.6,1)$ and $(1.4,-1)$, respectively. The path loss factor, β, is 2. $\mathcal{B}$ must be aware of the elements of the RLNC matrices, which range from [0.3, 0.5] for $\mathcal{A}$ and $\mathcal{R}$ to encode. The reference image

used at $\mathcal{A}$ and $\mathcal{R}$ is identical to image number 17 in Fig.2, while image number 13 is considered the estimated reference image at $\mathcal{E}$.

Fig. 2. Images for testing and validation of Proposed Protocol.

Fig. 3 and Fig. 4 show the PSNR and SSIM simulation results as a function of SNR (dB) in Rayleigh fading with a downscale factor of 10 ($\epsilon = 10$, meaning the transmission bandwidth is reduced by 10 times). The intersection of SRT and SDT is divided into two ranges (which depend on the position of the relay and will be examined in another article) called LR-SNR (Low Range SNR, i.e., below approximately 27 dB) and HR-SNR (High Range SNR, i.e., beyond approximately 27 dB). In the LR-SNR area, SRT performs better than SDT due to the help of the relay node in a high-noise environment. Overall, SCR outperforms both SRT and SDT. SCR is slightly better than SRT and significantly better than SDT in LR-SNR, while in HR-SNR, SCR is far superior to SRT and slightly better than SDT. $\mathcal{E}$'s recovery performance is extremely low compared to SCR, SRT, and SDT (below approximately 9-10 dB for PSNR and 25-35% for SSIM), which implies that $\mathcal{E}$ won't be able to retrieve the image $\mathcal{A}$ intended to send to $\mathcal{B}$. To improve SCR's performance, the number of relays can be increased. Fig.3 and Fig.4 demonstrate that by increasing the number of relays from 1 to 5 and 9, SCR is improved by approximately 0.2 and 0.4 dB for PSNR, and by 2.5% and 5% for SSIM.

V. Conclusions

In this paper, we have constructed a protocol for secure image cooperative communications in Rayleigh fading, where $\mathcal{A}$ wants to safely transfer HR images to $\mathcal{B}$ across two hops with the assistance of a relay. RLNC has been utilized at $\mathcal{A}$ and $\mathcal{R}$ (for security purposes) to prevent Eve from accessing the original image. The HR images at $\mathcal{B}$ are recovered from their LR equivalents using ISR. $\mathcal{A}$ downscaled the images (to save transmission bandwidth) before transferring them to $\mathcal{B}$ and $\mathcal{R}$. Simulation results have demonstrated that $\mathcal{E}$'s recovery

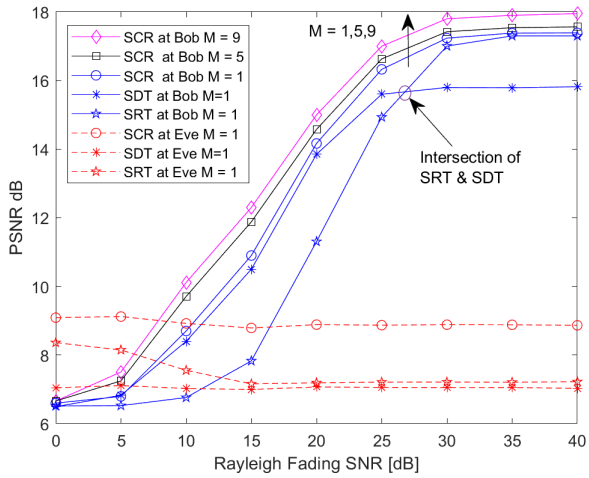

Fig. 3. PSNR with different Relay Selection.

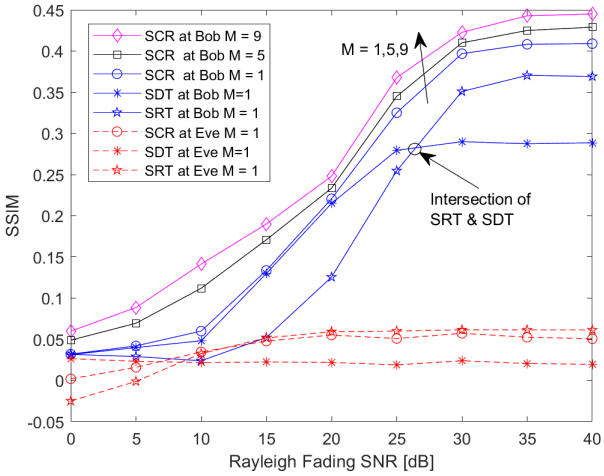

Fig. 4. SSIM with with different Relay Selection.

performance is significantly poor compared to that of SCR, SRT, and SDT. By utilizing relay selection strategies, we can improve SCR performance over the fading channel.

References

[1] Nosratinia, A., Hunter, T. & Hedayat, A. Cooperative communication in wireless networks. *IEEE Communications Magazine*. **42**, 74-80 (2004)

[2] Sendonaris, A., Erkip, E. & Aazhang, B. User cooperation diversity. Part I. System description. *IEEE Transactions On Communications*. **51**, 1927-1938 (2003)

[3] Bletsas, A., Khisti, A., Reed, D. & Lippman, A. A simple cooperative diversity method based on network path selection. *IEEE Journal On Selected Areas In Communications*. **24**, 659-672 (2006)

[4] Fareed, M. & Uysal, M. On relay selection for decode-and-forward relaying. *IEEE Transactions On Wireless Communications*. **8**, 3341-3346 (2009)

[5] Zhou, Z., Zhou, S., Cui, J. & Cui, S. Energy-efficient cooperative communication based on power control and selective single-relay in wireless sensor networks. *IEEE Transactions On Wireless Communications*. **7**, 3066-3078 (2008)

[6] Adam, H., Bettstetter, C. & Senouci, S. Adaptive relay selection in cooperative wireless networks. *2008 IEEE 19th International Symposium On Personal, Indoor And Mobile Radio Communications*. pp. 1-5 (2008)

[7] Nguyen, D., Tran, T., Nguyen, T. & Bose, B. Wireless broadcast using network coding. *IEEE Transactions On Vehicular Technology*. **58**, 914-925 (2008)

[8] Soljanin, E. LECTURE NOTES-Network Multicast with Network Coding. *IEEE Signal Processing Magazine*. **25**, 109 (2008)

[9] Ju, M. & Kim, I. Error performance analysis of BPSK modulation in physical-layer network-coded bidirectional relay networks. *IEEE Transactions On Communications*. **58**, 2770-2775 (2010)

[10] Lima, L., Médard, M. & Barros, J. Random linear network coding: A free cipher?. *2007 IEEE International Symposium On Information Theory*. pp. 546-550 (2007)

[11] Davis, G. & Danskin, J. Joint source and channel coding for image transmission over lossy packet networks. *Applications Of Digital Image Processing XIX*. **2847** pp. 376-387 (1996)

[12] Stuhlmuller, K., Farber, N., Link, M. & Girod, B. Analysis of video transmission over lossy channels. *IEEE Journal On Selected Areas In Communications*. **18**, 1012-1032 (2000)

[13] Kim, J., Lee, J. & Lee, K. Accurate image super-resolution using very deep convolutional networks. *Proceedings Of The IEEE Conference On Computer Vision And Pattern Recognition, Las Vegas, NV, USA*. pp. 1646-1654

[14] Wang, Z., Chen, J. & Hoi, S. Deep learning for image super-resolution: A survey. *IEEE Transactions On Pattern Analysis And Machine Intelligence*. **43**, 3365-3387 (2020)

[15] Kaur, M. & Kumar, V. A comprehensive review on image encryption techniques. *Archives Of Computational Methods In Engineering*. **27**, 15-43 (2020)

[16] Johnson, N., Duric, Z. & Jajodia, S. Information hiding: steganography and watermarking-attacks and countermeasures: steganography and watermarking: attacks and countermeasures. (Springer Science & Business Media, 2001)

[17] Duong, H., Phan, C., Vien, Q. & Nguyen, T. A Secure Cooperative Transmission of Image Super-Resolution in Wireless Relay Networks. *Electronics*. **12**, 3764 (2023)

[18] Ghaderi, J., Xie, L. & Shen, X. Hierarchical cooperation in ad hoc networks: Optimal clustering and achievable throughput. *IEEE Transactions On Information Theory*. **55**, 3425-3436 (2009)

[19] Zhang, K., Zuo, W., Chen, Y., Meng, D. & Zhang, L. Beyond a gaussian denoiser: Residual learning of deep cnn for image denoising. *IEEE Transactions On Image Processing*. **26**, 3142-3155 (2017)

[20] Grubinger, M., Clough, P., Müller, H. & Deselaers, T. The IAPR TC-12 benchmark: A new evaluation resource for visual information systems. *International Workshop OntoImage'2006 Language Resources For Content-Based Image Retrieval, Held In Conjunction With LREC'06, Genoa, Italy,*. **2, pp 13-23**

[21] Porter, T. & Duff, T. Compositing digital images. *Proceedings Of The 11th Annual Conference On Computer Graphics And Interactive Techniques*. pp. 253-259 (1984)

[22] Hore, A. & Ziou, D. Image quality metrics: PSNR vs. SSIM. *2010 20th International Conference On Pattern Recognition*. pp. 2366-2369 (2010)

[23] Wang, Z., Bovik, A., Sheikh, H. & Simoncelli, E. Image quality assessment: from error visibility to structural similarity. *IEEE Transactions On Image Processing*. **13**, 600-612 (2004)